UDC 669.15-194.55:620.172.251.226

STRUCTURAL CHANGES IN STEEL 10Kh9K3V1M1FBR DUE TO CREEP

A. Yu. Kipelova,[1] A. N. Belyakov,[2] V. N. Skorobogatykh,[1] I. A. Shchenkova,[2] and R. O. Kaibyshev[1]

The evolution of microstructure in steel 10Kh9K3V1M1FBR during creep and in aging at 600 – 650°C is studied. The results are compared with data for steel P91. The role of cobalt in growth in the long-term strength is considered.

Keywords: steels of martensitic class, creep, long-term strength, microstructure, mechanical properties.

INTRODUCTION

Steels of martensitic class with 9% Cr began to be used in boilers and steam conduits in the middle of the 1980s after the development of a steel certified by the ASME as P91 [1 – 3]. The possibility of long-term operation of steels of type P91 at 600°C was ensured by the stable dislocation structure of troostomartensite formed as a result of air hardening (normalizing) and medium-temperature tempering. In the Russian-language literature such tempering of steels of type P91 is still called high-temperature tempering, despite the absence of not only recrystallization but even cell formation in the dislocation structure of martensite. Stability of the dislocation structure in tempering and in creep of martensitic steels of the new generation is ensured by formation of nanosize dispersed particles of Me(C, N)-type carbonitrides [4] and $Me_{23}C_6$-type carbides [1, 4, 5]. Another important factor positively affecting the stability of the dislocation structure of troostomartensite is segregation of Fe_2W-type Laves phases [1, 5].

The success of steel P91 has led to the development of an improved version, i.e., steel E911 with operating temperature raised to 620°C due to the introduction of 1% W; this grade was certified by the ASME as P911 [2 – 3, 5, 6]. The operating temperature of steels of martensitic class can be increased still more by introduction of 3% Co [8 – 11]. The National Institute of Materials Science of Japan has used this approach for creating a series of martensitic steels with 9% Cr, which contain 3% Co [5, 8 – 10]. These steels have very high creep resistance, which has made it possible to certify them according to the ASME and METI (the Ministry of Economy, Trade and Industry of Japan) rules and to start their commercial use in power generating plants with steam temperature of 650°C. The Russian "TsNIITMASh" has used a similar approach for developing steel 10Kh9K3V1M1FBR bearing 3% Co, which is a modified version of grade 10Kh9V1M1FBR, the Russian counterpart of P911 [7]. Steel 10Kh9K3V1M1FBR developed at the "TsNIITMASh" is inferior to the grades developed at the National Institute of Materials Science of Japan with higher content of tungsten with respect to the parameters of long-term strength. At the same time, is has some process advantages compared to the martensitic steels with 3% W. From the standpoint of physical metallurgy the development of this steel has made it possible to determine the role of cobalt in the growth in high-temperature strength of steels of martensitic class, because its behavior in the creep and aging process can be compared with the behavior of P911 under similar conditions [6]. Such work cannot be performed for the steels with 3% W [5, 8 – 10, 11], because in the cobalt-free versions of these steels the specific volume of δ-ferrite ≥ 10% [8, 9]. For this reason the causes of the positive effect of cobalt on the high-temperature strength of martensitic steels with 9% Cr are still unclear.

Only the following facts can be mentioned as reliably established ones.

1. Introduction of copper, which is an effective γ-stabilizer equal to nickel in the effect on the critical points and on the temperature of the beginning of martensitic transformation [8], makes it possible to raise the content of W and Mo in the solid solution and to lower the total content $\Sigma(C + N)$ without formation of δ-ferrite. This ensures substantial growth in the long-term strength [5, 8 – 10] of martensitic

[1] Belgorod State University, Belgorod, Russia (E-mail: rustam kaibyshev@bsu.edu.ru).

[2] Central Research Institute for Machine Building Technology (GNTs RF OAO NPO "TsNIITMASh"), Moscow, Russia.

steels with 9 – 11% Cr. Consequently, the first result of the addition of cobalt is widening of the possibility to change the chemical composition of the high-chromium steels of martensitic class and thus to increase their creep resistance due to suppression of formation of δ-ferrite. Simultaneously, the addition of cobalt removes formation of retained austenite [8].

2. Cobalt is contained in the solid solution and is virtually absent in the $Me_{23}C_6$-type carbides and Laves phases segregated in aging and creep [9]. Its effect on the creep resistance is explainable by the fact that it lowers the rate of diffusion [12] and provides additional solid-solution hardening.

The aim of the present work consisted in studying the structural changes in creep of steel 10Kh9K3V1M1FBR and estimating the effect of cobalt on its phase composition by comparing the latter with the phase composition of cobalt-free steel P911.

METHODS OF STUDY

We studied high-temperature steel 10Kh9K3V3M1FBR with the following chemical composition (in wt.%): 0.13 C, 8.6 Cr, 3.2 Co, 1.2 W, 0.9 Mo, 0.1 Cu, 0.2 V, 0.07 Nb, 0.04 N, 0.005 B, 0.02 Mn, 0.05 Ni, 0.06 Si, remainder Fe. The test heats were melted at the "TsNIITMASh." The specimens for the creep tests were hardened in air from 1050°C and tempered at 750°C for 3 h. The creep tests were performed using lever-type machines produced at the "TsNIITMASh" for cylindric specimens 10 mm in diameter and design length of 50 mm. The tests conditions were (*1*) a stress $\sigma = 200$ MPa and a temperature $t = 600$°C and (*2*) $\sigma = 120$ MPa and $t = 650$°C. The first temperature is a standard operating one for steels of type P911 (10Kh9V1M1FBR) bearing no Co. The second temperature was considered to be the maximum operating one for the promising steel 10Kh9K3V1M1FBR. At 650°C additional creep tests in a stress range of 118 – 200 MPa were performed using an ATS2330 lever-type machine for flat specimens with a base of 25 mm and a cross section of 7 × 3 mm fabricated according to the ASTM E139-00 standard. The Vickers microhardness was measured in the central part of a specimen along its axis from the neck to the head with the help of an Affri "DM8" digital microhardness meter at a load of 5 N on the indenter.

The microstructure was studied for two specimens deformed until failure for about 4.5×10^3 h at a stress of 200 MPa ($t = 600$°C) and 120 MPa ($t = 650$°C). The structure was studied in the region of the neck (at a distance of about 1.5 mm from the place of failure) and in the head of the specimens using a FEI "Quanta 600F" scanning electron microscope (SEM) equipped with an image analyzer and an image sensor for detecting the diffraction of back-scattered electrons (EBSD) and a Jeol "JEM-2100" transmission electron microscope (TEM) with accelerating voltage of 200 kV. The maps of off-orientations were plotted with allowance for angular off-orientations exceeding 2°. The volume fraction and the size of the Fe_2W-type Laves phases were determined using SEM photographs in back-scattered electrons (*Z*-contrast) [13]. The volume fraction of the Laves phases was evaluated in terms of the specific fraction of their area on the cross sectional area of the specimen. In this regime the photographs of the Laves phases give a bright contrast, and the $Me_{23}C_6$ carbides give a contrast close to that of the matrix [13]. The size and the chemical composition of the Me(C, N)-type carbonitrides, of the $Me_{23}C_6$-type carbides, and of the Cr(Nb, V)N *Z*-phase were determined with the help of carbon replicas during the TEM study. The nature of the phases was determined from the results of a joint analysis of the diffraction patterns of the phases and of the data of the energy dispersive analysis performed using "INCA Energy TEM 250" attachments (Oxford Instruments). The fine structure was studied on foils obtained by the method of jet electrochemical polishing in a Struers "TenuPol-5" device using a 10% solution of perchloric acid in nitric acid as an electrolyte. The size of the subgrains was calculated by the method of random secants. The dislocation density inside martensite laths and subgrains was determined in terms of the number of the points of outcome of individual dislocations to the surface of the foil by the method of [14]. We used methods of structural analysis to study the aging processes occurring in the heads of specimens and the creep processes occurring in their functional parts. The error of the measurements did not exceed 8%.

The phase composition was simulated by thermodynamic computations using Thermo-Calc software and the TCFE4 data base.

RESULTS

Mechanical Properties. Figure 1 presents the dependence of the time before creep-induced failure on the stresses applied, which was obtained for steel 10Kh9K3V1M1FBR experimentally; for comparison, we also present the data for steel P911 from [2, 6]. It can be seen that the addition of 3% Co into steel P911 increases the time to failure by about a factor of 3 at 600°C and by almost a factor of 5 at 650°C. Thus, the introduction of 3% Co ensures significant growth in the long-term strength of steel P911 and the effect intensifies upon growth in the temperature.

Microstructure after Tempering. A typical microstructure formed in steel 10Kh9K3V1M1FBR after hardening from 1050°C and tempering at 750°C is presented in Fig. 2. The mean size of the initial austenite grains (IAG) is 14 μm, which is smaller than the size of the IAG (20.2 μm) in steel P911 [6]. This is connected with the fact that the temperature of heating of steel P911 for hardening in [6] was 1100°C. The transverse size of the laths of packet martensite after tempering is 370 nm. According to the data of the EBSD over 50% boundary off-orientations are large-angle ones

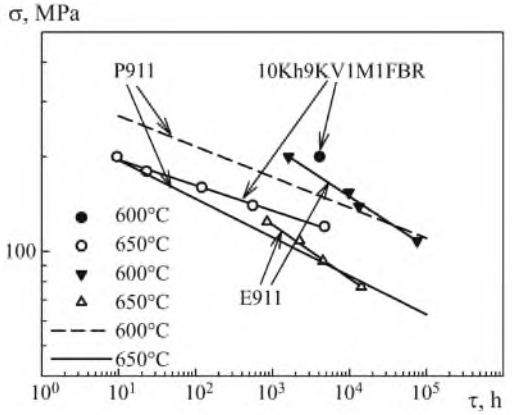

Fig. 1. Curves of long-term strength of steels P911 [2], E911 [6], and 10Kh9K3V1M1FBR: σ) applied stress; τ) time to failure.

(Fig. 2*b*) and 15% of the boundaries have crystallographic parameters that allow us to classify them as special boundaries in accordance with the Brandon criterion (Table 1). It should be noted that the data on the fraction of large-angle boundaries are somewhat overestimated, because the off-orientation maps have been plotted without allowance for the small-angle lath boundaries with off-orientation less than 2°. However, the method makes it possible to perform qualitative comparative analysis of the structural changes with high reliability, which is determined by the high rate of automatic processing of a large array of experimental points.

In the process of tempering, fine $Me_{23}C_6$-type carbides are segregated primarily over lath boundaries (Fig. 2*a*) and over the boundaries of blocks, packets, and IAG (Fig. 2*c*). The mean size of such segregations is 80 nm. The size of the $Me_{23}C_6$ particles segregated over the boundaries of IAG in steel 10Kh9K3V1M1FBR is twice lower than in steel P911 (see Fig. 3*a* in [6]). In contrast to steel P911 [6] we have not detected features of segregation of Me_2X-type carbides in steel 10Kh9K2V1M1FBR. Carbonitrides of type Me(C, N) with a mean size of 35 nm are uniformly distributed over the volume of steel 10Kh9K3V1M1FBR. It has been shown [15] that these carbonitrides are represented by two phases, i.e., niobium- and vanadium-enriched ones. Particles of type V(C, N) with plate shape 15 nm long and 2.5 nm thick are encountered. In steel P911 the mean size of the particles of Me(C, N) is substantially higher and ranges from 40 to 90 nm [6]. Note that the difference in the tempering modes of steels P911 (760°C for 2 h) and steel 10Kh9K3V1M1FBR cannot be the cause of the difference in the sizes of the carbides and carbonitrides.

The hardness of the steel after tempering is 250 *HV*, which is somewhat lower than the hardness of P911 (269 ± 2.4 *HV*) [6]. The study of the fine structure showed (Fig. 2*a* and *c*) a characteristic contrast inside martensite plates, which reflects the presence of long-acting internal fields of elastic stresses [16, 17].

Hardness and Microstructure after Testing for Creep. Aging for 4.5×10^3 h does not result in noticeable softening of the material. The hardness in the heads of the specimens is 255 and 244 *HV* after testing at 600 and 650°C, respectively. In steel P911 the hardness after similar holds is 270 and 245 *HV* [6]. The characteristics of the microstructure after the creep tests and after tempering for comparison are presented in Table 1. The electron microscope contrast on thin foils shows [16, 17] (Fig. 3*a* and *c*) that the long-acting fields of internal stresses in the troostomartensitic structure are preserved but are lower after aging. We observed a substantial decrease in the hardness in the neck of a specimen at $t = 650$°C (Fig. 4). This correlates with the disappearance of internal stresses in the fine structure after creep tests, which can be inferred from the results of TEM [16, 17] (Fig. 5*a* and *c*). At the same time, localization of plastic yielding near the fracture surface of a specimen tested at 600°C does not influence substantially the softening of the material. Despite the high gradient of plastic strain in the neck of the specimen the change in the hardness over it at a distance of 10 mm from the place of failure does not exceed 15%. It should be noted that though the microhardness in the necks of specimens of the studied steel and of steel P911 [6] is about the same after creep testing at 600°C, the microhardness in the necks of

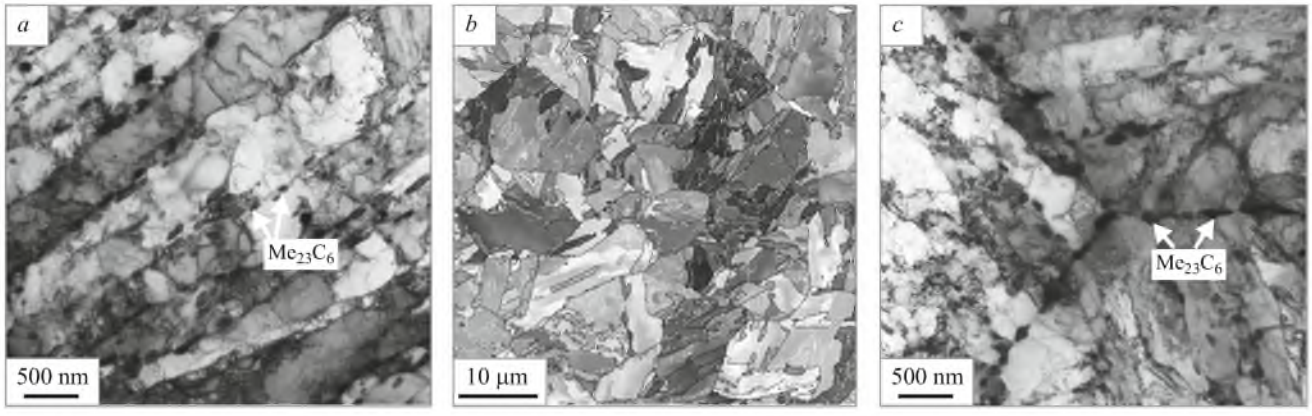

Fig. 2. Microstructure (*a*, *c*, TEM) and map of off-orientations (*b*) of steel 10Kh9K3V1M1FBR after 3-h tempering at 750°C.

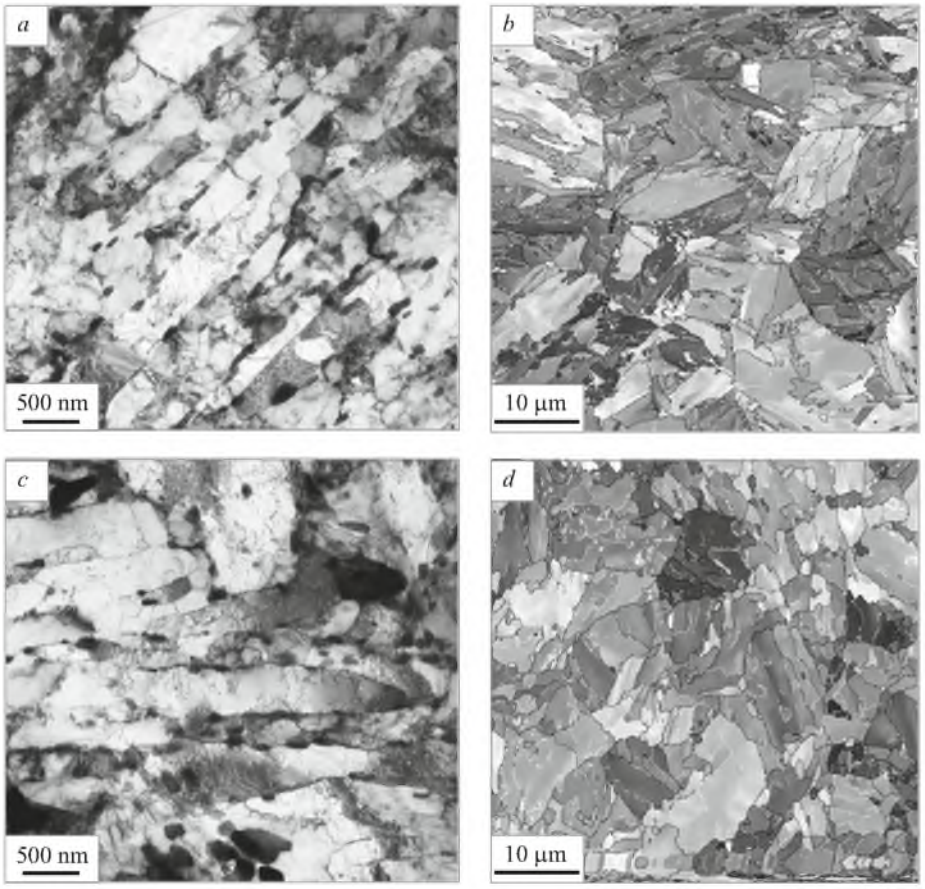

Fig. 3. Microstructure (*a*, *c*, TEM) and maps of off-orientations (*b*, *d*) for heads of specimens of steel 10Kh9K3V1M1FBR after testing for creep in the following modes: *a*, *b*) $t = 600°C$, $\sigma = 200$ MPa; *c*, *d*) $t = 650°C$, $\sigma = 120$ MPa.

specimens of steel 10Kh9K3V1M1FBR (160 *HV*) after creep testing at 650°C is 22% lower than in steel P911 (about 200 *HV*) [6] at comparable hold times.

Softening in the process of creep is accompanied by structural changes that are the most noticeable in the necks of specimens. The structure troostomartensite in the heads of the specimens changes little (Fig. 3, Table 1). The transverse sizes of the laths of martensite in the heads of the specimens are 510 and 560 nm after creep testing at 600 and 650°C, respectively (Table 1). Long-term aging has virtually no effect on the dislocation density at 600°C and about halves it at 650°C. Since the thickness of the martensite plates at the two aging temperatures is close and the dislocation density differs somewhat, we may assume that the growth in the thickness of the martensite plates at the two temperatures occurs by different mechanisms. It should also be noted that the fractions of large-angle and special boundaries in the heads of the specimens remain almost invariable after the aging (Table 1).

During the creep process the dislocation structure of the troostomartensite loses its packet morphology and is transformed into a conventional subgrain structure typical for

TABLE 1. Parameters of Microstructure of Steel 10Kh9V1M1FBR

Mode of heat treatment or testing	Studied region	d_m, nm	ρ, m^{-2}	d_s, nm	$\Sigma 3$, %	LAB, %
Hardening from 1050°C + tempering at 750°C	–	370	6.20×10^{14}	80	15.0	56
Creep at 600°C, 200 MPa, 4103 h	Neck	670	1.70×10^{14}	165	2.7	35
	Head	510	5.30×10^{14}	85	14.0	51
Creep at 650°C, 120 MPa, 4743 h	Neck	1300	0.46×10^{14}	165	3.2	29
	Head	560	2.86×10^{14}	125	7.3	50

Notations: d_m) mean size of laths/subgrains; ρ) density of lattice dislocations; d_s) mean size of secondary phases; $\Sigma 3$) fraction of special boundaries in which the number of metal lattice sites per one coinciding site in the common superlattice is equal to 3; LAB) fraction of large-angle boundaries.

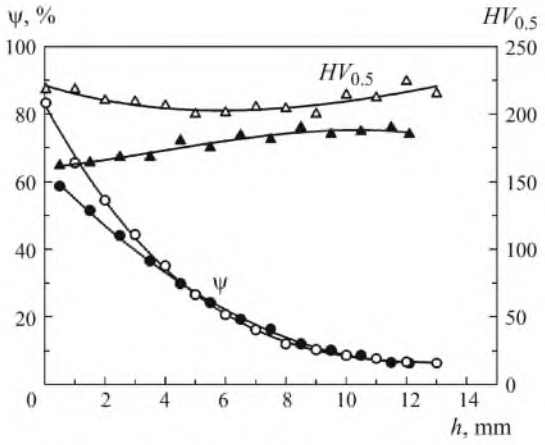

Fig. 4. Variation of the hardness and contraction over the length of specimens (h is the distance from the place of failure) for steel 10Kh9K3V1M1FBR after creep testing at 600°C, $\sigma = 200$ MPa (empty symbols) and 650°C, $\sigma = 120$ MPa (filled symbols).

thermal deformation [17] (Fig. 5). This transformation consists in rearrangement of dislocations inside dislocation boundaries, which leads to disappearance of the long-acting fields of elastic stresses (Fig. 5*a* and *c*). The size of the subgrains after the creep tests exceeds considerably the thickness of the laths in the troostomartensite (Table 1). The transverse sizes of the subgrains in the necks are 670 and 1300 nm after testing for creep at 600 and 650°C, respectively (Table 1). Decrease in the fraction of large-angle boundaries according to the data of the EBSD analysis (Table 1) reflects growth in the fraction of small-angle boundaries with off-orientation exceeding 2°. This means that the transformation of dislocation boundaries into subgrain ones and their subsequent migration increase their off-orientation. The higher the creep test temperature and the larger the size of the subgrains, the more small-angle boundaries acquire an off-orientation exceeding 2° (Table 1). In addition, the transformation of martensite laths into subgrains in the process of plastic yielding is accompanied by changes in the crystal geometry parameters of block boundaries. The fraction of special boundaries in the creep process at 600 and 650°C decreases to 3% (Table 1), which leads to a decrease in the fraction of the large-angle grain boundaries. This phenomenon has also been observed for other steels with 9% Cr. It has not been explained satisfactorily until present.

The cause of the deterioration of the stability of the dislocation structure of the troostomartensite and of the growth of subgrains in the creep process is coagulation of particles of secondary phases, the mean size of which increases by a factor of 2 (Table 2). The curve describing the size distribution of the particles of secondary phases shifts toward larger sizes (Fig. 6). However, the stability of the structure is af-

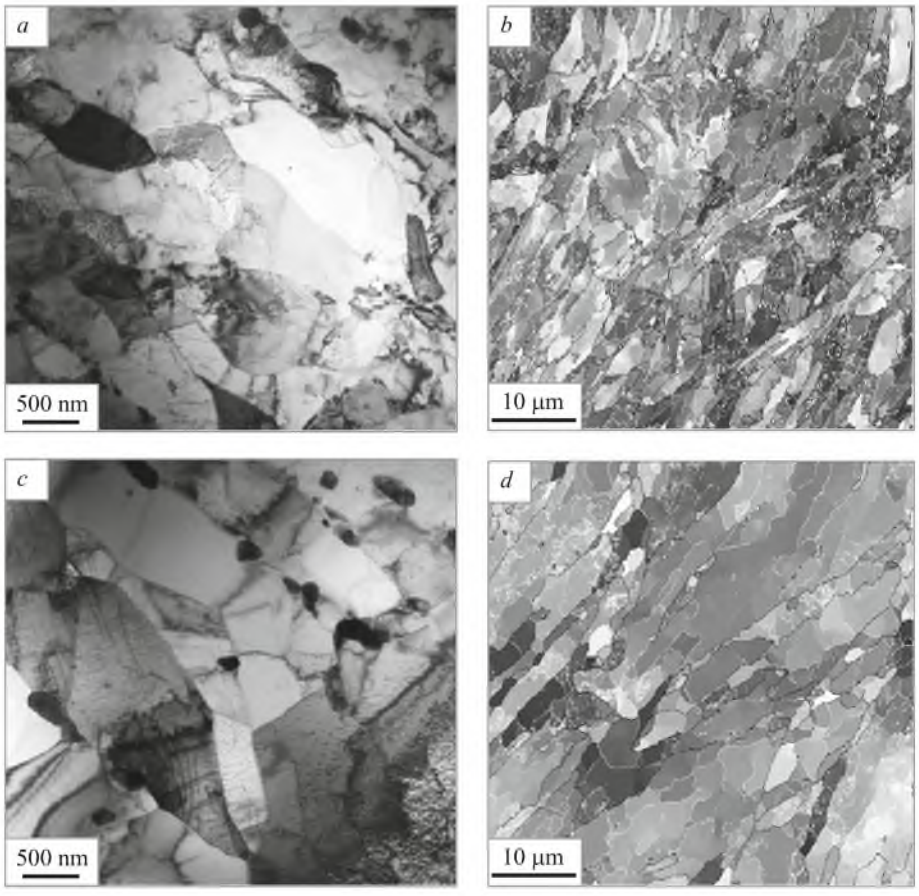

Fig. 5. Microstructure (*a*, *c*, TEM) and maps of off-orientations (*b*, *d*) for necks of specimens of steel 10Kh9K3V1M1FBR after creep tests performed in the following modes: *a*, *b*) $t = 600$°C, $\sigma = 200$ MPa; *c*, *d*) $t = 650$°C, $\sigma = 120$ MPa.

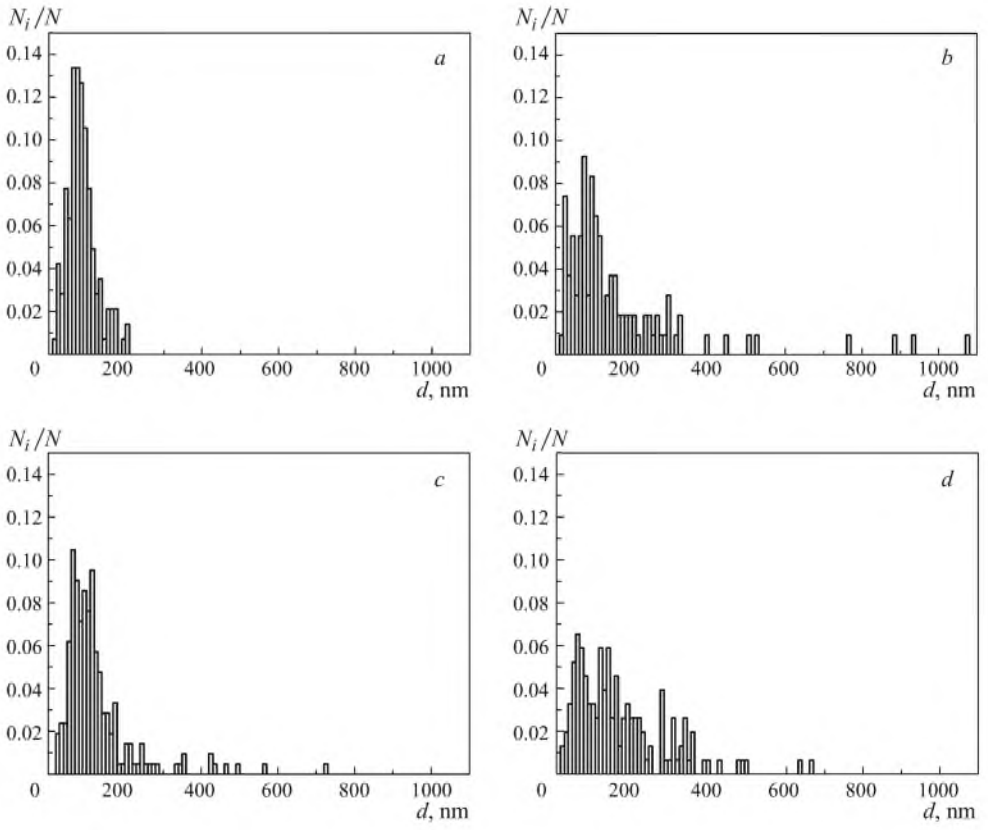

Fig. 6. Size distribution of carbides in heads (*a*, *c*) and necks (*b*, *d*) of specimens of steel 10Kh9K3V1M1FBR after creep tests performed in the following modes: *a*, *b*) $t = 600°C$, $\sigma = 200$ MPa; *c*, *d*) $t = 650°C$, $\sigma = 120$ MPa.

fected not only by the size of the secondary phases but also by their distribution over the volume of the matrix.

During aging, Fe_2W-type Laves phases segregate primarily over the boundaries of IAG and packets, i.e., over the large-angle boundaries (see Fig. 7*a* and *c*). In the process of creep all these phases are segregated additionally over block boundaries (Fig. 7*b* and *d*), i.e., after the creep the particles of the Laves phase are distributed more uniformly. Aging

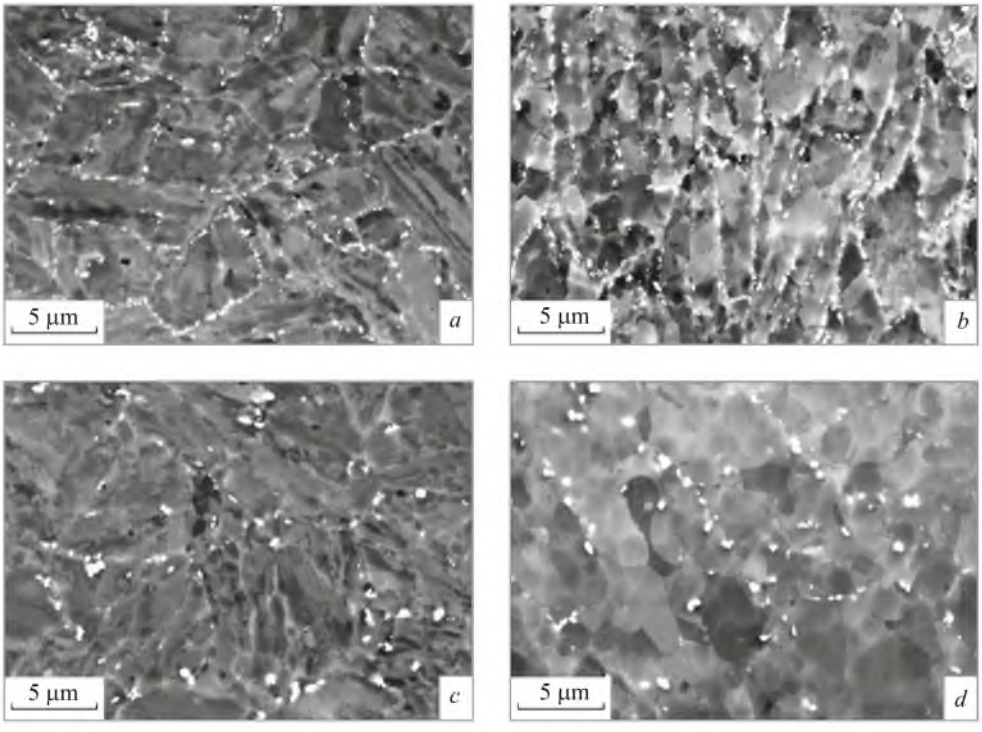

Fig. 7. Laves phases in the structure of steel 10Kh9K3V1M1FBR (SEM photographs obtained in the mode of *Z*-contrast) after creep testing in the modes: *a*, *b*) $t = 600°C$, $\sigma = 200$ MPa; *c*, *d*) $t = 650°C$, $\sigma = 120$ MPa; *a*, *c*) head; *b*, *d*) neck.

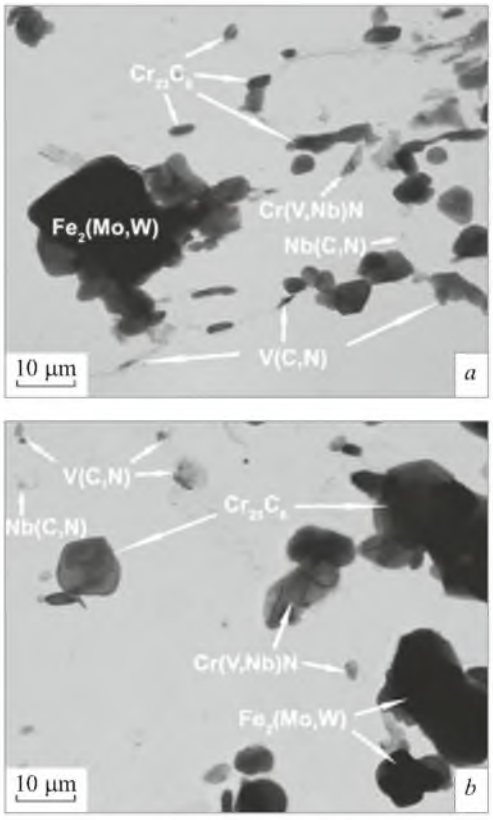

Fig. 8. Carbides, carbonitrides, and Laves phases in the head (*a*) and neck (*b*) of a specimen of steel 10Kh9K3V1M1FBR after testing for creep at 650°C (carbon replicas).

and creep reduce their size by a factor of 2 – 3 (Fig. 8, Table 2) as compared to the sizes of the Laves phases segregated in steel P911 [6] and their volume fraction is < 0.02. The chemical composition of the segregating Laves phases is characterized by the proportion Mo : W = 1 : 1 as in steel P911 [6]. The Laves phases contain 2.5% Co on the average.

The size of the Me(C, N) carbonitrides changes due to creep as a function of their chemical composition. Both the vanadium-enriched Me(C, N) carbonitrides and the niobium-enriched ones remain uniformly distributed over the volume of the metallic matrix. The size of the Nb(C, N)-base carbonitrides remains virtually unchanged after aging and even after creep at 650°C; the mean size of the V(C, N)-base carbonitrides after creep and aging increases (Fig. 8, Table 2). After aging at 600 and 650°C, just as after tempering, we observed dispersed particles of type V(C, N) with the shape of plates 15 nm long and 3.5 nm thick. After creep at these temperatures the major part of them coagulated and their mean size attained 40 – 60 nm (Fig. 8, Table 2). Note that in steel P911 coagulation of carbonitrides of type Me(C, N) has not been detected even after creep [6]. This may be connected with the fact that the size of the carbonitrides after tempering of steel P911 exceeded their size in steel 10Kh9K3V1M1FBR after creep at 650°C. The main reason for performing the tempering at a higher temperature [6] is the necessity to increase the size of the Me(C, N)-type carbonitrides, which are more resistant to creep-induced coagulation. This ensures a higher creep resistance after a hold for over 3×10^4 h than in the steel tempered at a lower temperature. These data show that in all probability the tempering temperature for steel 10Kh9K2V1M1FBR has been chosen too low and should be raised to 770 – 780°C.

Carbides of type $Me_{23}C_6$ grow both in aging and in creep (Fig. 6 – 8, Table 2). Aging at 600°C is an exception, when the mean size of these carbides decreases as a result of their additional segregation. Aging at 600°C does not cause intense coagulation of $Me_{23}C_6$-type carbides (Fig. 6*a*); at 650°C their coagulation causes formation of coarse carbides of type $Me_{23}C_6$ lying over IAG boundaries or packet boundaries (Fig. 6*c*, Fig. 8, Table 2). After aging, the $Me_{23}C_6$-type carbides have a chiefly equiaxed shape; some particles have the shape of plates with the ratio of the longitudinal size to the transverse one less than 3 : 1 (Figs. 3 and 8). Plate carbides are mostly positioned over boundaries of martensite crystals and boundaries of IAG. It should be noted that after aging most of the $Me_{23}C_6$ carbides that have formed after tempering over the boundaries of martensite crystals (Fig. 2) remain at their places.

Creep processes give rise to another situation; most of the plates of the $Me_{23}C_6$ carbides are arranged over large-angle boundaries (Fig. 5); intense coagulation of these carbides leads to the appearance of particles over 0.5 μm in size on IAG boundaries (Fig. 6*b* and *d*, Fig. 8, Table 2). The amount of carbides lying over subgrain boundaries decreases notice-

TABLE 2. Structural Parameters of Phases Contained in Steel 10Kh9K3V1M1FBR

Mode of heat treatment or testing	Studied region	Mean size of phases, nm			
		$Fe_2(Mo, W)$	$Me_{23}C_6$	VC	NbC
Hardening from 1050°C + tempering at 750°C	–	–	115	30	35
Creep at 600°C, 200 MPa, 4103 h	Neck	170 (1.9 %)	155	40	25
	Head	180 (1.5 %)	100	40	30
Creep at 650°C, 120 MPa, 4743 h	Neck	265 (1.7 %)	210	60	40
	Head	260 (1.8 %)	125	50	30

Note. The values in parentheses denote the volume fraction of the $F_2(Mo, W)$ phase in %.

ably. The size of carbides of type $Me_{23}C_6$ on the IAG and packet boundaries increases (Fig. 5). Consequently, coagulation in the creep processes increases the size of the $Me_{23}C_6$ carbides that had greater a size after tempering as a result of their heterogeneous nucleation on large-angle boundaries, whereas the carbides that had a lower size after tempering dissolve, because the places of their segregation were dislocation boundaries of martensite crystals. As a result, the volume fractions of the $Me_{23}C_6$-type carbides with equiaxed shape and with plate shape are about equal after creep. Such coagulation of the $Me_{23}C_6$-type carbides removes the force hindering the migration of subgrain boundaries. Analysis of the experimental data presented in [6] shows that the mean size of $Me_{23}C_6$-type carbides in steel P911 after aging and creep is about a factor of 1.5 larger than in steel 10Kh9K3V1M1FBR.

In contrast to steel P911 we have not detected Me_2C-type carbides in steel 10Kh9K3V1M1FBR either after creep or after aging. At the same time, we detected a *Z*-phase (Fig. 8). After aging at 650°C the particles of Cr(Nb, V)N had a shape of plates about 30 nm thick and up to 200 nm long. This allows us to assume that a part of its phase boundaries have a coherent or semicoherent nature [18]. After creep at 650°C we observed round particles of the *Z*-phase the size of which varied from 40 to 200 nm. In steel P911 the size of the *Z*-particles after creep even at 600°C was larger than in steel 10Kh9K3V1M1FBR at 650°C and amounted to 200 – 350 nm. Note that the formation of the *Z*-phase in steel 10Kh9K3V1M1FBR does not lead to a considerable decrease in the volume fraction of Me(C, N) carbonitrides, the dispersed particles of which were encountered at a small distance from the *Z*-phase (Fig. 8). Particles of type Nb(C, N) (Fig. 8), which should be the first to dissolve upon formation of a *Z*-phase [18], were also encountered.

DISCUSSION

Structural Changes in Creep. The results of our study show unambiguously that the nature of the variation of the dislocation structure of martensite in aging and creep of steel 10Kh9K3V1M1FBR are determined by the change in the size, volume fraction, and nature of particles of the secondary phases. The head of the specimen after testing preserves the structure of troostomartensite at inconsiderable growth of the laths both at 600°C and at 650°C, while the neck acquires a subgrain structure. The size of the subgrains d and the density of the intragrain dislocations ρ in the neck correlates well with the yielding stress σ, i.e., $\sigma \sim d^{-1} \sim \sqrt{\rho}$.

The main role in the stabilization of the dislocation structure in creep belongs to the carbonitrides of type Me(C, N); in aging, a substantial contribution to the deceleration of the migration of subgrain boundaries is also made by $Me_{23}C_6$-type carbides. The force hindering the migration due to the Me(C, N)-type carbonitrides and $Me_{23}C_6$-type carbides arranged over the dislocation boundaries turns out to be enough for preventing the transformation of the dislocation structure of troostomartensite into a subgrain one even after aging for 4×10^3 h. In creep, if the volume fraction and the mean size of the Me(C, N)-type carbonitrides changes inconsiderably (at 600°C), even the transformation of the dislocation boundaries of troostomartensite into subgrain ones does not lead to their intense migration despite the dissolution of the $Me_{23}C_6$-type carbides deposited on them after tempering. As a result, the evolution of the structure in the process of creep at 600°C consists primarily in the rearrangement of the dislocation boundaries of martensite into subgrain ones. The main difference of dislocation boundaries from subgrain ones is the absence of long-acting fields of elastic stresses in the latter. The carbonitrides of type Me(C, N), which are located uniformly over the volume of the material, cannot prevent such transformation. However, they are able to decelerate or suppress the migration of subgrain boundaries in the case where their size has changed inconsiderably (Table 2). Migration of the boundaries of subgrains formed at the place of martensite crystals is hindered by the $Me_{23}C_6$ carbides lying over these boundaries until their dissolution and by the Me(C, N) carbonitrides uniformly distributed over the metallic matrix. At 650°C the dissolution of V(C, N) carbonitrides in the form of plates 2.5 nm thick and the growth in the mean size of these carbonitrides by a factor of 2 (Table 2) reduce the hindering force to a value at which the subgrain boundaries start to migrate intensely. Dynamic cell formation develops in steel 10Kh9K3V1M1FBR [14, 19, 20]. The lowering of the precipitation hardening by nanosize carbonitride particles and of the hardening introduced by the dislocation structure of the troostomartensite leads to accelerated creep and failure of the material. Thus, in order to prevent the development of dynamic cell formation in the structure of the troostomartensite and, accordingly, to raise the operating temperature of the steel, it is necessary to prevent the dissolution of the coagulation-induced $Me_{23}C_6$-type carbides located over subgrain boundaries and the coagulation of the V(C, N) carbonitrides.

Segregation and coagulation of Laves phases over the boundaries of blocks, packets and IAG cannot affect the migration of former boundaries of martensite crystals. However, the Laves phases together with the $Me_{23}C_6$ carbides lying over the boundaries of the IAG, packets, and blocks suppress the migration of large-angle boundaries virtually completely and thus prevent the development of recrystallization. The opinion that the nanosize particles of Laves phases freshly segregated from the solid solution in the creep process can suppress the rearrangement of dislocations in the dislocation boundaries of martensite before they start to coagulate [21] has not been confirmed by the results of our structural studies. It should be noted that the volume fraction of the Laves phases has turned out to be virtually the same (about 1.8%) within the error of measurement at the studied temperatures both after aging and after creep (Table 2). This amount corresponds approximately to the values of the equi-

librium volume fraction of the Laves phases obtained by thermodynamic computations, i.e., a Laves phase is segregated in accordance with the equilibrium diagram. However, it is segregated heterogeneously. Creep increases the number of places of heterogeneous nucleation of the Laves phase at the expense of the boundaries of blocks, which prevents growth in their size in creep. This reduces the evolution of the dislocation structure of the troostomartensite in creep to growth in the size of the subgrains formed at the place of martensite crystals. It should be noted that at the relatively low volume fraction of the Laves phases the dominant part of tungsten and molybdenum remains in the solid solution. This ensures the high creep resistance of the steel [1].

Effect of Cobalt on the Creep Resistance. Analysis of experimental data on the evolution of microstructure in the studied steel and in steel P911 shows that the positive effect of cobalt is a result of its action on the rate of diffusion and on the process of segregation of Laves phases from the solid solution. Deceleration of the rate of diffusion as a result of the addition of 3% Co not only lowers the rate of the creeping dislocations but, what is the most important, decelerates the coagulation of dispersed carbides and carbonitrides as well as the segregation and coagulation of Laves phases in the processes of creep and aging. This makes it possible to preserve the force decelerating the migration of subgrain boundaries at a sufficient level, which prevents the development of dynamic cell formation in steel 10Kh9K3V1M1FBR at higher temperatures than in steel P911 [6]. Thermodynamic simulation of the effect of the cobalt content on the equilibrium phase composition of a Fe – 9% Cr – 1% Mo steel has shown that growth in its content virtually does not change the ultimate solubility of tungsten in the solid solution in a temperature range of 600 – 650°C. The most probable explanation of the lower size of the Laves phases in the steel with 3% Co with respect to steel P911 [6] is the deceleration of the diffusion of metallic atoms in the solid solution as a result of the introduction of cobalt. In addition, the introduction of cobalt into steel P911 suppresses the segregation of the Me_2C carbide, which is susceptible to intense coagulation in creep [6].

The introduction of 3% Co affects the formation of the *Z*-phase, which is the most undesirable with respect to the creep resistance of high-chromium steels [20]. The causes of the finer size of the *Z*-phase in the steel with cobalt as compared to P911 are unclear. We may only suggest that the positive factors are the cobalt-induced deceleration of the diffusion and the possible action of cobalt on the driving force of the nucleation of the phase. It should be stressed that the long-term strength and the changes in the microstructure due to creep with long holds ($\geq 3 \times 10^4$ h) should be studied for cobalt-bearing steels with utmost care before starting their commercial use in order to estimate the possible degradation of the creep resistance as a result of formation of the *Z*-phase.

Thus, the introduction of 3% Co into a martensitic steel with 9% Cr increases substantially its creep resistance due to the improvement of the structural stability. Additional alloying with cobalt is an effective means for raising the operating temperature of thermotechnical steels.

CONCLUSIONS

1. Additional alloying of steel of type P911 (10Kh9V1M1FBR) with cobalt in an amount of 3% has made it possible to increase the time to failure in creep tests performed at 600 – 650°C by a factor of 3 – 5.

2. The microstructure of troostomartensite in steel 10KhK3V1M1FBR is preserved almost without change in the process of long-term aging (over 4000 h) at a temperature of 600 – 650°C. In creep tests under similar temperature and time conditions the structure in the necks of the specimens transforms from troostomartensite into a coarse subgrain structure. The size of the subgrains is 670 and 1300 nm after testing for creep at 600 and 650°C respectively. The coarsening of the substructure is a result of the growth of secondary carbides and Laves phases.

3. In steel 10Kh9K3V1M1FBR at 600 and 650°C the mean size of the Nb(C, N) carbonitrides remains virtually unchanged. After creep and aging at 600°C the size of the particles of V(C, N) remains virtually invariable, whereas the creep and the aging at 650°C increases their size from 30 to 60 nm.

4. The processes of aging and creep cause formation of a Cr(Nb, V)N *Z*-phase in steel 10Kh9K3V1M1FBR. However, this does not result in catastrophic dissolution of carbonitrides of type Me(C, N).

This work been performed with financial support of the Federal Agency for Science and Innovations, Grant No. 02.523.12.3019. The authors are grateful to the Collective Use Center "Diagnostics of Structure and Properties of Nanomaterials" of the Belgorod State University for supplying them with the equipment for structure studies and mechanical tests and to the Chief of the Department of the Physical Metallurgy of Nonferrous Metals of the Moscow Institute for Steel and Alloys A. N. Solonin for the possibility to work with the Thermo-Calc software.

REFERENCES

1. R. O. Kaibyshev, V. N. Skorobogatykh, and I. A. Shchenkova, "New steels of martensitic class for heat power engineering. High-temperature properties," *Fiz. Met. Metalloved.*, **109**(2), 200 – 215 (2010).
2. Landolt-Bornstein, "Creep properties of heat resistant steels and superalloys Group VIII," *Adv. Mat. Tech.*, **2B**, 144 – 149 (2003).
3. J. C. Vaillant, B. Vandenberghe, B. Hahn, et al., "T/P23, 24, 911 and 92: new grades for advanced coal-fired power plants – properties and experience," *Int. J. Press. Vess. Piping*, **85**, 38 – 46 (2008).
4. N. F. Lashko, L. V. Zaslavskaya, M. N. Kozlova, et al., *Physicochemical Phase Analysis of Steels and Alloys* [in Russian], Metallurgiya, Moscow (1978).

5. F. Abe, M. Taneike, and K. Sawada, "Alloy design of creep resistant 9Cr steel using a dispersion of nano-sized carbonitrides, *Int. J. Press. Vess. Piping*, **84**, 3 – 12 (2007).
6. G. Qin, S. V. Hainsworth, A. V. Strang, et al., "TEM studies of microstructural evolution in creep exposed E911," in: *Creep & Fracture in High Temperature Components, 2nd ECCC Creep Conf.*, DEStech Publications (2009), pp. 889 – 899.
7. A. V. Dub, V. N. Skorobogatykh, V. S. Dub, et al., "High-temperature steel, RF Patent No. 2333287, 26.09.2006," *Byull. Izobr. Polezn. Modeli*, No. 25 (2008).
8. L. Helis, Y. Toda, T. Hara, H. Miyazaki, and F. Abe, "Effect of cobalt on the microstructure of tempered martensitic 9Cr steel for ultra-supercritical power plants, *Mater. Sci. Eng.*, **A510 – 511**, 88 – 94 (2009).
9. K. Yanada, M. Igarashi, S. Muneki, and F. Abe, "Effect of Co addition on microstructure in high Cr ferritic steels," *ISIJ Int.*, **43**(9), 1438 – 1443 (2003).
10. M. Taneike, F. Abe, and K. Sawada, "Creep-strengthening of steel at high temperatures using nano-sized carbonitride dispersions," *Nature*, **424**, 294 – 296 (2003).
11. F. Abe, "Analysis of creep rates of tempered martensitic 9% Cr steel based on microstructural evolution," *Mater. Sci. Eng.*, **510 – 511**, 64 – 69 (2009).
12. Landolt-Bornstein, "Numerical data and functional relationships in science and technology – new series," *Diffusion Solid Met. Alloys*, **26**, 51, 298, 347 – 249 (1990).
13. G. Dimmler, P. Wenert, E. Kozeschnik, and H. Cerjak, "Quantification of the Laves phase in advanced 9 – 12% Cr steels using a standard SEM," *Mater. Char.*, **51**, 341 – 352 (2003).
14. R. Kaibyshev, K. Shipilova, F. Musin, and Y. Motohashi, "Continuous dynamic recrystallization in an Al – Li – Mg – Sc alloy during equal-channel angular extrusion," *Mater. Sci. Eng.*, **396**, 341 – 351 (2005).
15. K. Suzuki, S. Kumai, Y. Toda, et al., "Two-phase separation of primary MX carbonitride during tempering in creep resistant 9Cr1MoVNb steel," *ISIJ Int.*, **43**(7), 1089 – 1094 (2003).
16. A. Belyakov, K. Tsuzaki, Y. Kimura, and Y. Mishima, "Tensile behavior of submicrocrystalline ferritic steel processed by large-strain deformation," *Philos. Mag. Lett.*, **89**, 201 – 212 (2009).
17. A. Belyakov, T. Sakai, H. Miura, and R. Kaibyshev, "Substructures and internal stresses developed under warm severe deformation of austenitic stainless steel," *Scr. Mater.*, **42**, 319 – 325 (2000).
18. H. K. Danielsen and J. Hald, "On the nucleation and dissolution process of *Z*-phase Cr(V, Nb)N in martensitic 12% Cr steels," *Mater. Sci. Eng.*, **A505**, 169 – 177 (2009).
19. A. Belyakov, R. Kaibyshev, V. Dudko, et al., "Effect of heat treatment on microstructure of a 9% Cr steel," in: *Creep & Fracture in High Temperature Components, 2nd ECCC Creep Conf.*, DEStech Publications (2009), pp. 1038 – 1045.
20. A. Belyakov, Y. Kimura, and K. Tsuzaki, "Microstructure evolution in dual phase stainless steel during severe deformation," *Acta Mater.*, **54**, 2521 – 2532 (2006).
21. F. Abe, "Effect of fine precipitation and subsequent coarsening of Fe_2W Laves phase on the creep deformation behavior of tempered martensitic 9Cr – W steels," *Metall. Mater. Trans.*, **36A**, 321 – 332 (2004).